Spatio-temporal Quantification of Deforestation and Understanding its Impact on Basin Hydrology-An attempt to Ensure Long-term Sustainability

Triparna Sett[1], Bhaskar R. Nikam [2*], Vaibhav Garg [3] and Praveen K. Thakur [4]

[1]PhD Scholar, Indian Institute of Remote Sensing, ISRO, Dehradun, India
[2]Scientist/Engineer 'SF', EDPO, Indian Space Research Organisation Headquarters, Bengaluru, India
[3]Scientisst/Engineer 'SF', Indian Institute of Remote Sensing, ISRO, Dehradun, India
[4]Scientist/Engineer 'SG', Indian Institute of Remote Sensing, ISRO, Dehradun, India
(*Corresponding author: bhaskarnikam@isro.gov.in)

ABSTRACT

The anthropogenic activities are the major drivers for global Land Use and Land Cover Change (LULCC), which in-term influences the behavior of hydrological system. Understanding the repercussions of historical LULCC may facilitate in charting the sustainable path for future development and management endeavors. In the present study, LULC of the Tel Basin, India, was mapped and LULCC was quantified using remote sensing data. LULC mapped during years 1985, 1995, 2005, & 2015 was compared to understand the sptio-temporal dynamics of changes occurred during last thirty years. A noteworthy reduction of -8.20% in forest cover was observed, associated with increases of 7.82% and 0.32% in agricultural and settlement, respectively. To decipher the impact of these LULCCs, notably deforestation and urbanization, on the hydrological behavior of the basin the Variable Infiltration Capacity (VIC) model was setup using remote sensing derived topographical, LULC, vegetation parameters along with the in-situ datasets on soil & meteorology. The model was calibrated-validated using observed hydrological data and employed to quantify the impact of LULCC on runoff, evapotranspiration (ET), and baseflow in the Basin. The results indicated reduction in evapotranspiration by 1.63% (167.48mm) from 1985 to 2015, while runoff and baseflow exhibited increment of 1.15% (67.33mm) and 3.87% (108.25mm), respectively. These changes appear to be mainly driven by the transformation of 1,600 km^2 of forest cover into agricultural and settlement land. The reduction of deep-rooted vegetative cover impels the reduction in permanent interception, ET and water holding capacity of the subsoil in the area, which further fuels the increase of surface runoff and baseflow from the basin. The pixel level analysis of LULCC and its impact on the hydrological behavior in the Tel Basin provides valuable inputs for the strategic management of water resources within the Basin, thereby contributing to informed decision-making for assuring long-term, environmental, socio-economic sustainability.

Keywords: LULC Change, Variable Infiltration Model, Tel Basin, hydrological modeling, sustainability.

1. INTRODUCTION

Land Use and Land Cover Change (LULCC) serves as a pivotal indicator of environmental transformations, contributing significantly to complex earth-atmosphere interactions (Gashaw et al. 2018). This phenomenon plays a substantial role in shaping hydrological and watershed processes (Garg et al. 2019; Naha, Rico-Ramirez, and Rosolem 2021), with anthropogenic factors serving as primary drivers of alterations in Land Use Land Cover (LULC). The consequential impacts extend across various hydrological processes within a watershed, encompassing interception, baseflow, evapotranspiration, surface runoff, percolation, groundwater recharge, water quality, and sediment yield. Numerous studies have delved into the effects of LULCC on hydrological processes (Garg et al., 2012; Garg et al., 2017; Aboelnour et al. 2021; Berihun et al. 2019; Ghimire et al. 2021; Matlhodi et al. 2021; Sulamo, Kassa, and Roba 2021), particularly highlighting the impacts of deforestation.

In this context, hydrological models play a crucial role in simulating complex hydrological processes. The Variable Infiltration Capacity (VIC) model, a semi-distributed macroscale land surface/hydrological model developed by Liang et al. (1994, 1996) and Cherkauer et al. (2003), operates on a grid-based system, employing an energy and water balance approach to solve hydrological processes. Renowned for its ability to accurately capture streamflow processes and all components of the water budget, the VIC model has gained widespread acceptance and utility in global hydrological studies across diverse climatic regions and spatial scales (Aggarwal et al., 2013; Aggarwal et al., 2016; Dixit et al., 2015; Shiradhonkar et al., 2015; Garg et al., 2016; Abdulla et al. 1996; Chen et al. 2018; Cuo et al. 2013; Dahri et al. 2021; Haddeland, Skaugen, and Lettenmaier 2006; Lee, Kim, and Wang 2022; Lohmann, Raschke, and Lettenmaier 1998; Maurer et al. 2002; Niemeyer et al. 2018; Nijssen et al. 1997; Nijssen, Schnur, and Lettenmaier 2001; Niu, Chen, and Sun 2015; Shayeghi, Azizian, and Brocca 2020; Shrestha et al. 2012; Su et al. 2016; Tavakoly et al. 2017; Vetter et al. 2015; Voisin et al. 2011; Wang et al. 2021; Zamani Sabzi et al. 2019). Additionally, the Indian subcontinent has witnessed numerous studies employing the VIC model to analyze the interplay of LULCC and climate change on hydrology (Keerthiga et al., 2017; Sharma et al., 2019; Aggarwal et al. 2012; Chandu, Eldho, and Mondal 2022; Dadhwal, Aggarwal, and Mishra 2010; Das et al. 2018; Garg et al. 2019; Garg et al. 2013; Garg et al. 2017, 2012; Hengade and Eldho 2019; Kumari et al. 2021; Nikam et al. 2018; Patidar and Behera 2019; Sinha, Eldho, and Subimal 2020; Naha, Rico-Ramirez, and Rosolem 2021).

Tel catchment, a sub-basin of Mahanadi River basin, in India has experienced severe impacts from droughts and flash floods (Verma, Patel, and Choudhari 2022; Verma et al., 2022). Most of the previous studies in this area have focused on drought assessment (Mishra and Nagarajan 2011), flood frequency analysis (Guru and Jha 2015) and morphometric analysis (Verma, Patel, and Choudhari 2022). Notably, studies combining geospatial technology and a semi-distributed model in the Mahanadi basin are limited (Behera et al. 2017; Behera et al. 2018; Dadhwal, Aggarwal, and Mishra 2010; Naha, Rico-Ramirez, and Rosolem 2021). Consequently, this study represents the inaugural attempt to investigate long-term hydrological behaviour changes (1981-2018) resulting from the extensive impact of deforestation in the Tel basin at a spatial resolution of 5 km. The primary objectives of this study are (1) LULC change detection and analysis employing machine learning techniques, and (2) quantifying the impacts of LULCC on hydrology of the basin.

2. MATERIAL AND METHODS

2.1. Study Area

The Tel River, is a prominent tributary of the Mahanadi River. Longitudinally the Tel sub-basin extends between 82° 03' E to 84°17' E, and north-south expansion of the sub-basin is covered between latitudes of 19° 15' N to 20°55' N. The catchment area of the Tel sub-basin encompasses 22,818 km^2, with the gauging station at Kesinga representing runoff output from 11,960 km^2 catchment and the gauging station at Kantamal having contributing area of 19,600 km^2 (Guru and Jha 2015). Characterized by a tropical wet and dry climate, the Tel sub-basin experiences an average annual rainfall of 1360 mm, with temperatures ranging from 14℃ to 40℃. The region encounters a distinct dry period from December to May due to the absence of rain from the northeast monsoon. The erratic rainfall pattern renders the area susceptible to frequent crop failures and drought conditions. Given the limited duration of water availability in the sub-basin, it becomes imperative to explore whether changes in Land Use and Land Cover (LULC) impacts the basin hydrology.

Agriculture assumes a dominant role in the Tel sub-basin, with paddy cultivation emerging as a major grain crop. The agricultural landscape also includes the cultivation of gram, mung, pea, mustard, and sugarcane. The sub-basin hosts semi-evergreen forest, tropical dry deciduous forest, tropical moist deciduous forest, mixed forest, and mangrove forest. Additionally, shrubland, grassland, and plantations contribute to the diverse land use mosaic within the sub-basin. The location of Tel sub-basin within the Odisha, India, its surface elevation profile and its appearance as seen during Oct.-Dec 2015 in the Slandered false colour composite generated using Landsat-8 OLI data, are shown in Figures 1 a to d.

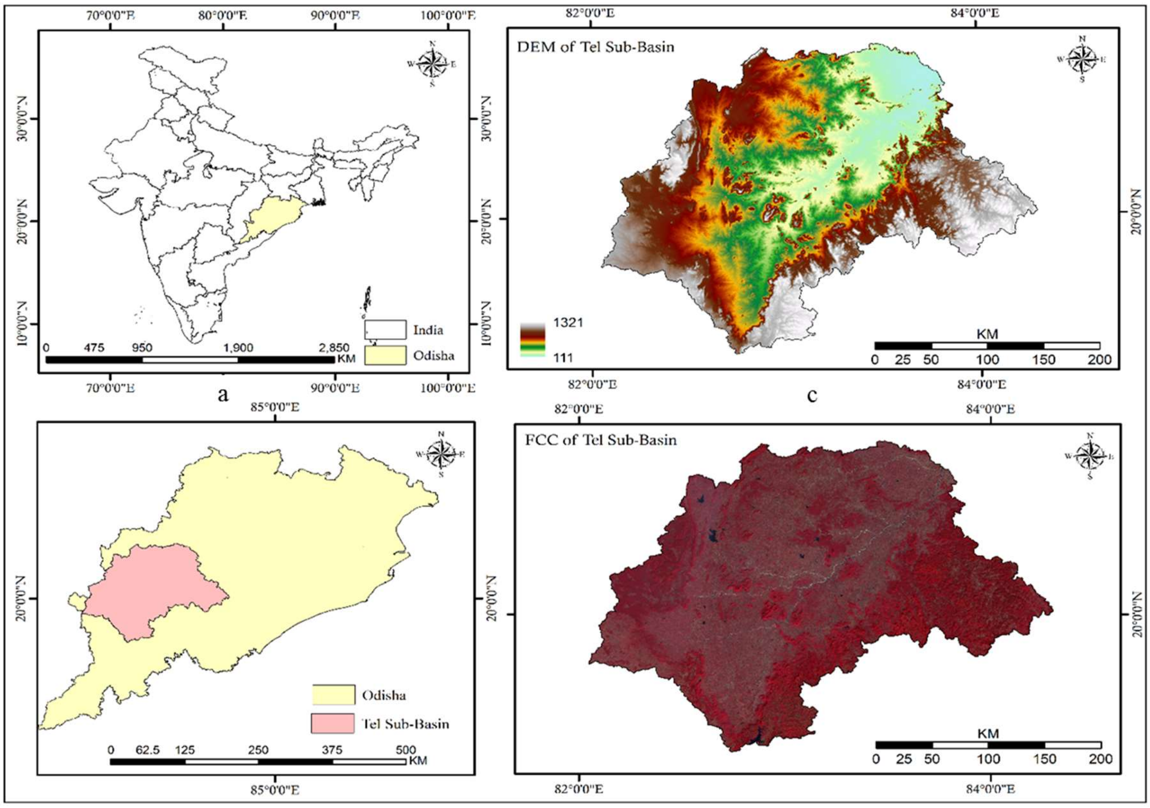

b d

Figure 1. **a)** Location of Odisha in India; **b)** location of Tel sub-basin in Odisha; **c)** DEM of Tel sub-basin; **d)** FCC image of Tel Basin (acquired date-01/10/2015-30/12/2015)

2.2. Assessment of LULC change

The LULC data of the Tel sub-basin for years 1985, 1995, and 2005 were sourced from India's Decadal Land Use and Land Cover Classifications maps (Roy et al., 2016). For the year 2015, a LULC map was generated utilizing Landsat 8 Operational Land Imager (OLI) data with a spatial resolution of 30m, acquired between 01/10/2015 and 30/12/2015. Leveraging the Google Earth Engine platform, various machine learning algorithms, including Decision Tree (DT; Quinlan, 1986), Support Vector Machine (SVM; Cortes and Vapnik, 1995), and Random Forest (RF; Breiman, 2001), were explored. Machine learning algorithms were chosen for their high accuracy and efficiency in classification tasks, with Random Forest identified as the most accurate classifier for this study. Knowledge based corrections in each iterations were performed to improve the classification accuracy of this exercise. The LULC of 2015 generated using machine learning tools was validated using reference data generated from legacy LULC maps and high resolution remote sensing data from year 2015. The integration of machine learning algorithms and rigorous correction processes underscores the commitment to precision in characterizing the evolving landscape over the specified temporal scale. The temporal analysis of LULC changes were performed at both sub-basin scale as well as pixel scale to quantify the LULC changes in the Tel sub-basin.

2.3. Hydrological Model

In this study, the Variable Infiltration Capacity (VIC) model was configured and validated for the Tel sub-basin, operating in a water balance mode. Specifically, the VIC-3L model, version 4.2.d, featuring three soil layers, was employed at a daily time step with a grid size of $0.05° \times 0.05°$. The VIC model necessitates comprehensive data on topography, soil characteristics, vegetation attributes, and the biophysical properties of the vegetation for each grid. To facilitate model input, various parameter files, including soil parameter file, vegetation parameter file, vegetation library file, and meteorological forcing files, were utilized. The vegetation parameterization in the VIC model encompasses critical factors such as monthly Leaf Area Index (LAI), albedo, displacement height, roughness length, stomatal and architectural resistances, and the fractional coverage of each LULC class within each grid cell. LAI and albedo, derived from remote sensing data, are particularly influential parameters that significantly impact the model performance. Additionally, the distribution of roots across soil layers for all vegetation classes, as outlined by Maurer et al. (2001a, 2001b), was incorporated in the vegetation parameterization, along with the percentage coverage of each LULC class within each active grid. The vegetation library file contained detailed information regarding the biophysical properties of each LULC class. Surface runoff in the VIC model is induced through the Xiangjiang formulation (Zhao, 1980), which enacts infiltration excess in the top two soil layers. Baseflow is generated using the Arno formulation from the third soil layer (Franchini and Pacciani, 1991). To determine the outflow from the basin, the VIC model is coupled with a separate routing model developed by Lohmann et al. (1996). The routing model utilizes an instantaneous unit hydrograph to direct runoff and baseflow to the grid cell edges, subsequently transporting them to the river/channel network through a linearized St. Venant equation. The routing model adheres to a straightforward river routing scheme.

For a comprehensive understanding of the model's formulations and structural features, one may refer to the works of Liang et al. (1996), Gao et al. (2010), and Liang et al. (1994b). Details about input preparation and model implementation can be referred from Garg et al. (2017), Nikam et al. (2018), Behara et al. (2019). The integration of these model components allows for a detailed and dynamic representation of the hydrological processes within the Tel sub-basin, facilitating the investigation of the impact of LULCC on the water balance over time.

2.4. Input Dataset for Hydrological Modelling

The VIC model incorporates several critical input parameters, encompassing soil type, land cover information, topographic features, and meteorological forcing, including rainfall, maximum and minimum temperatures, and wind speed. To populate these parameters for the Tel sub-basin, a comprehensive dataset was generated. Decadal LULC data for the years 1985, 1995, and 2005 were obtained from the Decadal Land Use and Land Cover Classifications across India (Roy et al., 2016), providing a spatial resolution of 100m. Topographic features were derived from Shuttle Radar Topography Mission (SRTM) elevation data, specifically the SRTM V3 product (SRTM Plus) provided by NASA JPL at a resolution of 1 arc-second, equivalent to 30 m (Farr et al., 2007). The meteorological data, including daily gridded precipitation, temperature, and wind speed, were sourced from the Copernicus Climate Data Store, offering ERA-5 data at a resolution of 27.83 km. The soil texture information for each grid cell was extracted from the Harmonized World Soil Database, accessible through the FAO Soils Portal. Utilizing the soil hydraulic properties index proposed by Cosby et al. (1984) and Reynolds et al. (2000), essential hydraulic parameters such as saturated hydraulic conductivity, porosity, field capacity, and wilting point were calculated for each soil type. Monthly leaf area index (LAI) data for each LULC class was obtained from the MODIS LAI data product (MCD15A2, 2005) at a spatial resolution of 500 m.

To validate the model, the observed daily discharge data at Kantamal gauging station for the period 1980 to 2018 was obtained from the India-Water Resources Information System (India-WRIS) portal. This compilation of diverse datasets ensures that the VIC model is well-trained for all the prevailing conditions in the Tel sub-basin, allowing for robust simulations and meaningful insights into the hydrological dynamics. The integration of observed discharge data further enhances the model's reliability and provides a basis for validating the simulated hydrological outputs.

2.5. Calibration and Validation of VIC Model

Calibration the VIC model was achieved by strategically tuning six key soil parameters: depth of three soil layers (d_1, d_2, d_3), infiltration shape parameter (bi), the fraction maximum subsurface flow where non-linear baseflow begins (D_S), and the fraction of maximum soil moisture where non-linear baseflow occurs (W_s) were utilized. The parameter *bi*, representing infiltration capacity, governs the partitioning of precipitation into infiltration and direct runoff. Higher value of *bi* leads to increased surface runoff and reduced infiltration. The parameters d_1, d_2, and d_3 denote the thickness of the first, second, and third soil layers, respectively. These parameters influence water availability for transpiration and baseflow, with thicker soil layers having a more significant impact on evapotranspiration, baseflow, and subsurface runoff. The parameters D_s and W_s relate to baseflow, determining the storage and release of water in the soil's lowest layer. Lower D_s values result in increased baseflow at lower soil moisture levels, while higher W_s values require more water for baseflow and contribute to a delayed peak runoff. To account for variations in vegetation characteristics over the years (e.g., 1985, 1995, 2005, and 2015), the vegetation parameters were adjusted annually. The simulated discharge from the model was compared against observed discharge data obtained from the India-WRIS portal to assess model performance.

The calibration process aimed to achieve optimal model performance, and Nash-Sutcliffe Efficiency (NSE) values of 0.80 was taken as reference to classify the model performance as satisfactory in the Tel sub-basin, following the guidelines set by ASCE (1993). The modle simulation period covers the time period from 1980 to 2018, ensuring consistency in climatological forcing. Out of total duration calibration phase spanned from 1985 to 2005, while validation was conducted over data from 1996 to 2018. Notably, NSE values of 0.85 and 0.80 were obtained for the calibration and validation periods, respectively. These values attest to the model's effectiveness in replicating observed discharge patterns and highlight its reliability in capturing the hydrological behaviour of the Tel sub-basin.

2.6. Analysis of the Impact of LULCC on hydrology using multiple scenarios

The impact of LULCC on hydrology (runoff potential, evapotranspiration, and baseflow) of the sub-basin was evaluated through a comparative analysis across four distinct scenarios:

- Scenario-1 (S1): Hydrological simulations based on LULC of year 1985, utilizing meteorological data spanning the period of 1980-2018.
- Scenario-2 (S2): Hydrological simulations based on LULC of year 1995, utilizing meteorological data spanning the period of 1980-2018.
- Scenario-3 (S3): Hydrological simulations based on LULC of year 2005, utilizing meteorological data spanning the period of 1980-2018.

- Scenario-4 (S4): Hydrological simulations based on LULC of year 2015, utilizing meteorological data spanning the period of 1980-2018.

By exposing four LULC scenarios (S1 to S4) to constant meteorological forcing (meteorological data of 1980-2018) the impact of climatic variations on the hydrological outputs were nullified. In S1 to S4 the variations if the hydrological behaviour of model will solely due to changes in surface conditions (LULC) in the basin. Through a meticulous analysis the changes in each hydrological component are quantified as either positive or negative anomalies in relation to a reference period. Quantification of these anomalies offers a means to detect and characterize spatial changes in hydrological processes caused due to changes in LULCC of the area. By systematically comparing the outcomes of each scenario against the backdrop of changing land cover, the study aims to elucidate the nuanced effects of LULCC on key hydrological parameters. This approach facilitates a comprehensive understanding of the intricate interplay between land use changes and the resulting alterations in water balance components over time.

3. RESULT AND DISCUSSION

3.1. LULC Mapping, accuracy assessment and Change Detection

The decadal LULC maps for 1985, 1995 and 2005 were taken from legacy data (Roy et al., 2016), however, the LULC for the year 2015 was derived using three machine learning algorithms (Decision Tree, DT; Support Vector Machine, SVM; and Random Forest, RF). The accuracy assessment was conducted to evaluate the LULC mapping performance of different Machine Learning (ML) for the year 2015. The results of the assessment are presented in Table 1, showcasing the overall accuracy and Kappa coefficients for each ML algorithm.

It is evident from the LULC accuracy assessment results that three ML algorithms employed for LULC mapping of Tel sub-basin Random Forest (RF) achieves highest mapping accuracy with overall accuracy of 95.69% and Kappa coefficient of 0.85.

Table 1. Results of accuracy assessment of LULC mapping using ML algorithms

ML Algorithm	Overall accuracy	Kappa coefficient
DT	74.01%	0.63
SVM	83.03 %	0.74
RF	95.69%	0.85

In the current investigation, decadal LULC maps were utilized to quantify the temporal evolution of land cover in the Tel sub-basin, with the year 1985 serving as the baseline. The LULC maps of year 1985, 1995, 2005 and 2015 are depicted in Figure 2. Two distinct analytical approaches were employed: (a) assessing overall changes in each LULC class relative to the baseline LULC of 1985, and (b) discerning the spatial patterns of LULC transformation at pixel level (100 m). The area occupied by each LULC class in 1995, 2005, and 2015 were compared against the reference year of 1985. This facilitated the calculation of the percentage change in total area under each LULC class with reference to baseline scenario (LULC of 1985). Through this approach, the study aimed to identify and characterize both spatial and temporal changes in LULC patterns, offering crucial insights into the spatio-temporal dynamics of LULC and LULCC in the study area. The results of this analysis are depicted in Figures 3a and 3b, employing False Color Composite (FCC) images to showcase the prominent changes that have occurred in the LULC classes. This nuanced exploration of LULC changes contributes to a broader comprehension of the interactions between human activities and the natural environment within the Tel sub-basin. The subsequent phases of the study are expected to delve into the hydrological implications of these LULC changes, shedding light on how alterations in land cover influences hydrology the region.

The analysis of Land Use and Land Cover Change (LULCC) between 1985 and 2015 in the Tel sub-basin has provided valuable insights into the evolving landscape over the past three decades. The key findings of this analysis include:

Forest Cover Changes (1985-2015): Forest cover exhibited a significant decline of 8.20% over the 30-year period. Approximately 1,600 km^2 of forest land underwent conversion to agricultural use (Table 3b), reflecting substantial deforestation to support the economic activity in the sub-basin.

Agricultural Expansion (1985-2015): Agriculture witnessed a noteworthy increase of 7.08%. On the other hand, around 122 km^2 of agricultural land was converted into water bodies, primarily due to the construction of water-retaining structures.

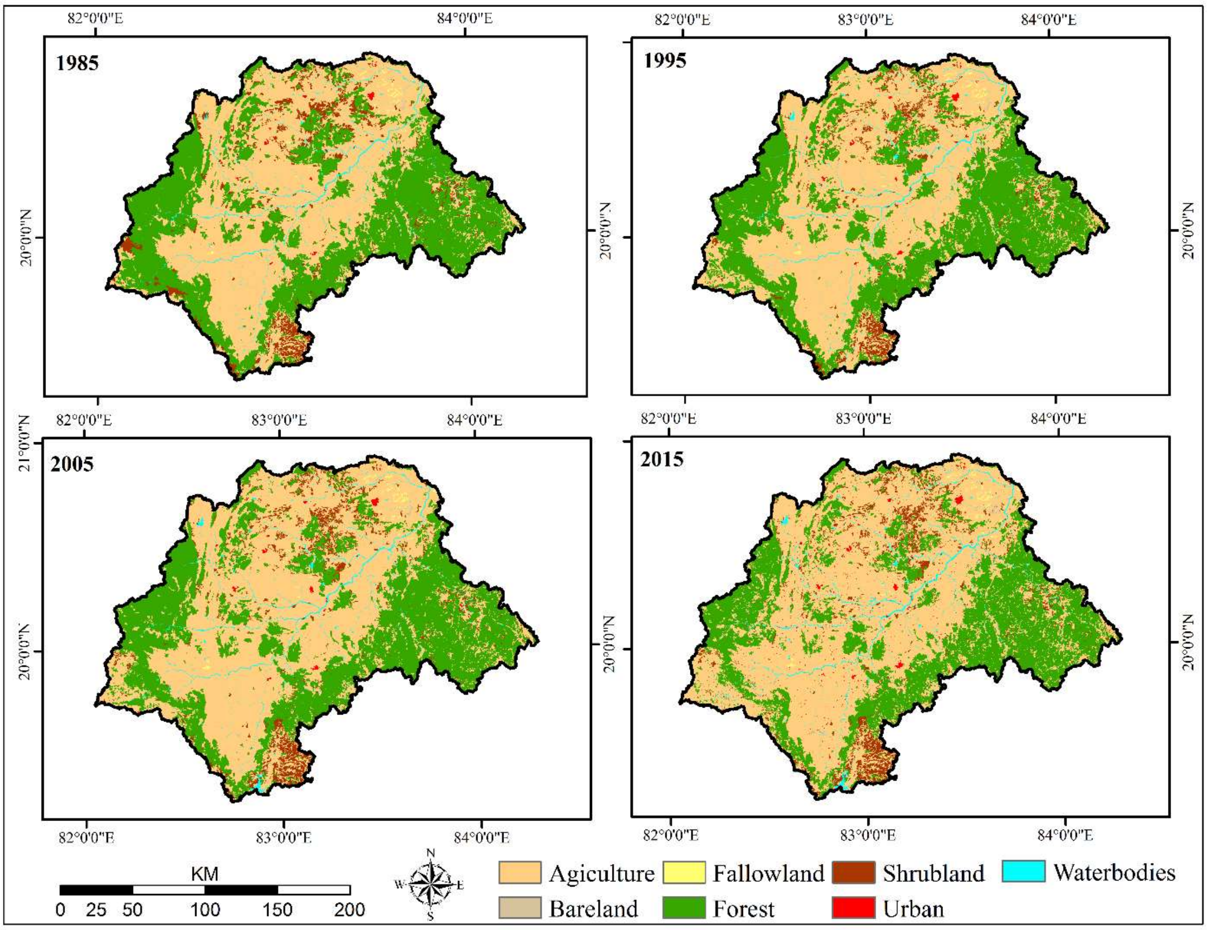

Figure 2. LULC maps of the basin for the years 1985, 1995, 2005, and 2015

Table 2 a. The LULC changes (km^2) matrix during year 1985 and 2005

		LULC of 2005							
		AG	**BL**	**FL**	**F**	**SL**	**UR**	**WB**	**Total**
LULC of 1985	**AG**	**11552.88**	1.70	8.01	671.45	454.79	2.96	77.18	12768.98
	BL	4.56	**9.77**	0.00	6.24	12.17	0.00	0.19	32.94
	FL	18.97	4.13	**36.58**	0.13	2.62	0.00	0.06	62.48
	F	162.15	0.48	0.05	**8658.33**	59.92	0.07	10.59	8891.59
	SL	115.12	0.74	0.16	312.04	**724.10**	0.06	3.49	1155.72
	UR	13.34	0.00	0.00	8.23	0.17	**35.65**	0.01	57.41
	WB	104.34	0.00	0.04	17.95	12.54	0.05	**233.06**	367.99
	Total	11971.36	16.82	44.84	9674.39	1266.32	38.79	324.58	**23337.11**

Table 2 b. The LULC changes (km^2) matrix during year 1985 and 2015

		LULC of 2015							
		AG	BL	FL	F	SL	UR	WB	Total
LULC of 1985	AG	**11473.02**	1.27	6.77	1607.76	467.56	2.11	65.46	13623.94
	BL	4.97	**10.02**	0.00	6.22	12.53	0.00	0.28	34.01
	FL	36.31	4.24	**37.73**	1.78	3.28	0.04	0.85	84.24
	F	59.78	0.27	0.03	**7701.10**	21.71	0.03	3.02	7785.94
	SL	176.92	0.89	0.19	325.16	**746.74**	0.06	4.59	1254.55
	UR	66.09	0.00	0.00	8.22	0.21	**36.50**	0.10	111.11
	WB	154.94	0.17	0.13	26.10	13.74	0.06	**250.30**	445.43
	Total	11972.03	16.86	44.84	9676.32	1265.78	38.80	324.59	**23339.22**

***The diagonal values for respective LULC classes are given in bold, indicating the area that has stayed unaltered between two time periods;*

Expansion of Settlements (1985-2015): Area under settlements has experienced a modest increase of 0.32%, this limited development of settlements can be attributed to the population rise and partial industrialisation/commercialization in the parts of sub-basin.

Fallow Land and Water Bodies (1985-2015): Increase of 0.17% was observed in the fallow land in the basin, suggesting migration of farmers to other sources of income (industry or other employments). Area under Water bodies has expanded by 0.51%, mainly attributed to the creation of water-retaining structures to meet growing population and industrial needs.

The analysis further highlighted distinct shifts in LULC between 1985 and 2005, with less pronounced changes compared to the period between 1985 and 2015. The apparent transformation observed from 1985 to 2015, particularly the conversion of a significant forest area to agriculture, shrub land, barren land, and fallow land, underscores the impact of developmental activities in the region.

Figures 3a and 3b illustrates the transformation of LULC, indicating how specific areas transitioned from one LULC class to another between 1985 and 2015. Figure 3a shows the LULC map of year 1985. Two regions, one on eastern part of sub-basin, indicated by black dashed box and another on western part of the sub-basin, indicated by red dashed box, are used to highlight these areas where dominant deforestation has occurred. The Standard FCC of these selected areas, generated using Landsat 5 TM data of year 1985 are also shown in Figure 3a . Similar, pectoral representation of LULC of the sub-basin for the year 2015 and the FCC images of selected areas are shown in Figure 3b. The substantial loss of forest cover can be clearly seen in the western part of the basin (red dashed box). The same can be seen in FCCs of year 1985 and 2015 of this part of the basin. On the other corner (black dashed box) no major change in forest boundary is observed, however the quality of forest cover/forest density appears to be degraded in 2015 compared to the 1985. This visual depiction allows for a clearer understanding of the spatial patterns and trends in land cover changes over the three-decade period.

The subsequent step in our analysis aimed at verifying the land conversion dynamics over a span of 30 years, from 1985 to 2015. A conversion map detailing the transitions between different LULC classes during this period was generated, providing a visual representation of the alterations in the landscape (see Figures 4).

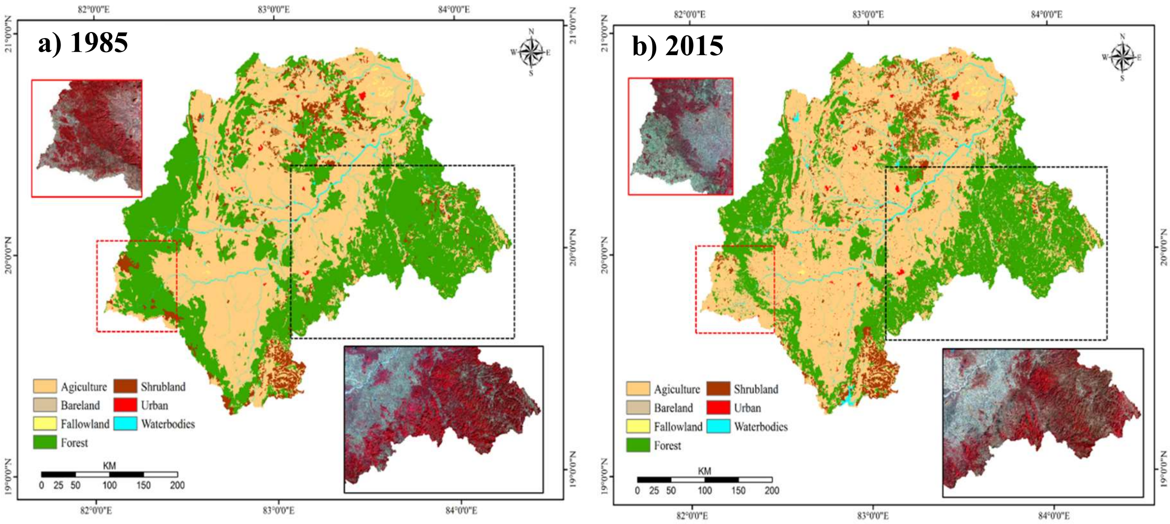

Figure 3.**a)** LULC and FCC image of selected area from year 1985; **b)** LULC and FCC image of selected area from year 2015

3.3 Impact of LULC change on basin hydrology

The hydrological response of Tel sub-basin under four LULC scenario (S1:1985; S2:1995; S3:2005; and S4:2015) under constant meteorological inputs were simulated using calibrated and validated VIC model. The hydrological components *viz.* evapotranspiration (ET), surface runoff, and baseflow under these four scenario were compared at basin level to quantify the overall impact of LULC changes that are highlighted in the previous sections. The key findings are as follows:

Increase in Surface Runoff Potential: The study observed a consistent increasing trend in average annual surface runoff potential of the basin. The long-term average annual surface runoff from the Tel sub-basin under Scenario S1 (LULC of year 1985) was around from 349.00

mm which increased to 353.00 mm under the Scenario S4 (LULC of year 2015). This suggests a potential shift in the basin's hydrological dynamics influenced by LULCC.

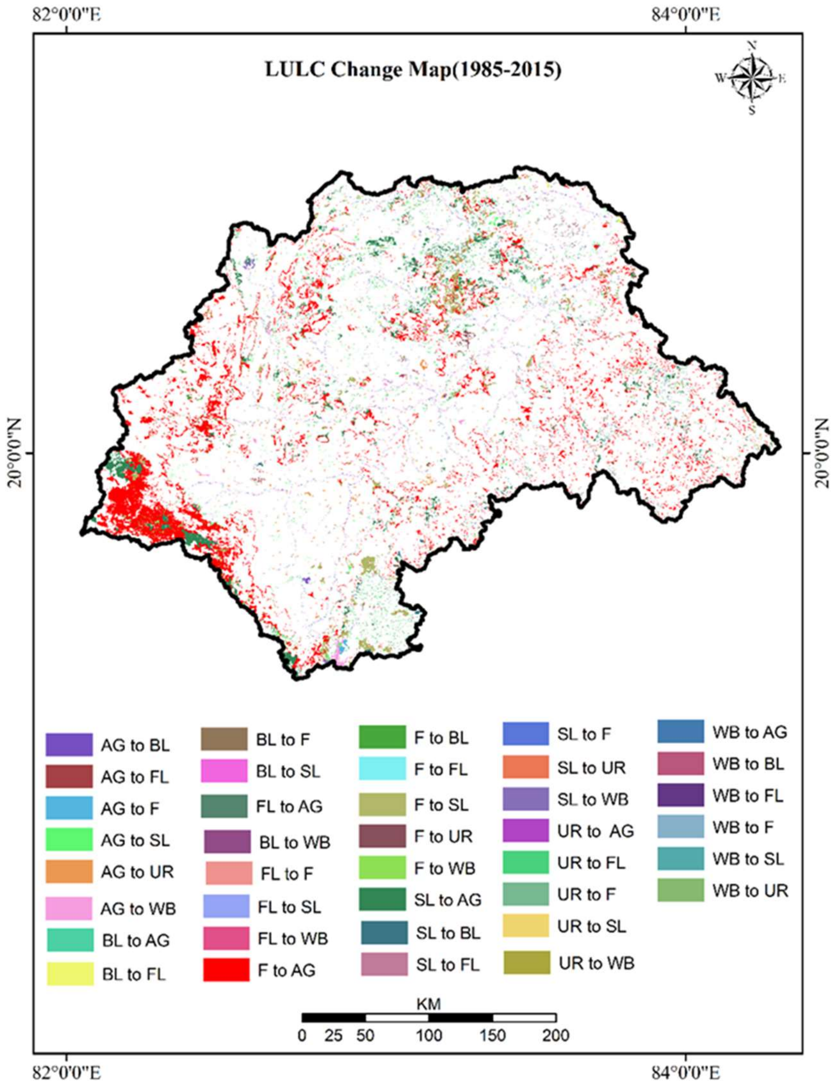

Figure 4. LULC conversion map of the basin between 1985 and 2015
AG- Agriculture, BL- Barren land, FL- Fallow land, F- Forest, SL-Shrubland, UR- Urban, WB – Waterbodies)

Evapotranspiration (ET) Changes: Contrary to the trends observed in case of surface runoff from the basin a noticeable decreasing trend in annual ET was observed from S1 (931.3 mm) to S4 (916.1 mm). This declining trend is in agreement with the LULCC trend of the sub-basin, reduction of permanent green.

Baseflow Increase: The study reveals a consistent increase in average baseflow from S1 (188.50 mm) to S4 (195.8 mm). This upward trend suggests alterations in land use impacting the groundwater recharge and subsurface flow dynamics.

The basin average values of surface runoff, evapotranspiration and baseflow under all four scenarios (S1, S2, S3, and S4) are summarised in Table 3 and depicted in Figures 5.

Table 3. Basin-average values of surface runoff, Evapotranspiration, and Baseflow under four LULC scenarios

	S1 (LULC- 1985)	**S2 (LULC-1995)**	**S3 (LULC-2005)**	**S4 (LULC-2015)**
Surface Runoff	349.0	350.0	351.7	353.0
Evapotranspiration	931.3	928.9	925.1	916.1
Baseflow	188.5	189.9	192.0	195.8

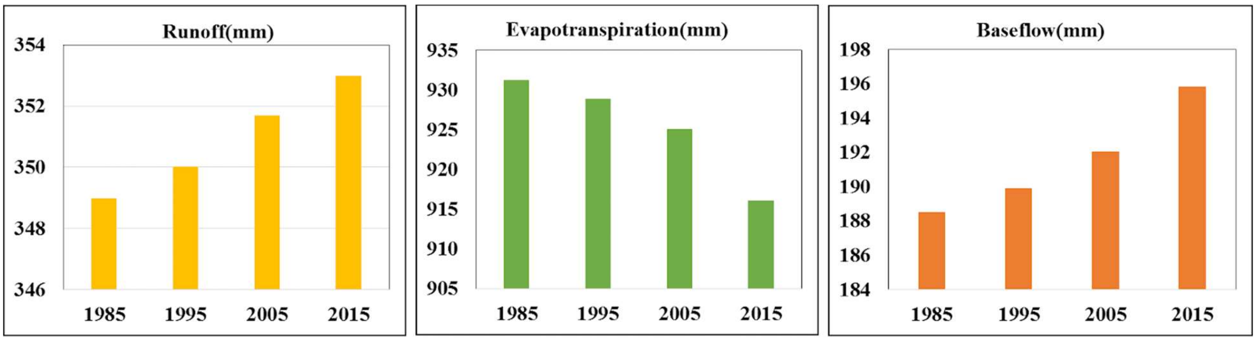

(A) (B) (C)

Figure 5. Trends in Surface runoff, Evapotranspiration, and Baseflow under four LULC scenario

It was observed that during the period of 30 years (1985 to 2015) the basin has undergone substantial changes in its LULC (e.g. ~8.2% reduction in forest cover, ~7% increase in active agriculture area, enhancement of waterbodies, etc.), however, the hydrological outputs under these LULC scenarios at sub-basin level show moderate to little variation (e.g. 4 mm increase in annual runoff, 15 mm reduction in annual evapotranspiration, etc.). Though even single millimetre change in any hydrological value over a basin as large as Tel sub-basin (22,818 km^2) is statistically substantial, however, the 1600 km^2 reduction of forest cover was expected to yield large hydrological response in the impact analysis results. The dampened impact of this LULCC on the hydrological behaviour insisted the need for in-depth analysis to find the causative factors. To understand this hydrological behaviour of Tel basin the pixel wise LULCC map (Figure 4) was converted into three classes 1) LULC change that has potential of increasing surface runoff, 2) LULC change that can potentially reduce the surface runoff, and 3) the class where not LULC change has happed. This classified map is shown in Figure 6. A careful analysis of this map revels that in the Tel sun-basin during 1985 to 2015 around 2143.71 km^2 area has undergone LULCC that has potential of reducing the surface runoff and at the same time around 848.57 km^2 area has undergone LULCC that can potentially increase the runoff response. This is why the surface runoff at basin scale appears to have dampened impact of LULCC from 1985- 2015. Most of the runoff acceleration impact due to conversion of permeable area into non-permeable area gets cancelled out by the large conversion of LULC classes that may reduce the runoff generation in the sub-basin. This self-cancelling behaviour of LULCC in any hydrological unit needs in-depth analysis and understanding to plan sustainable future/developmental activities.

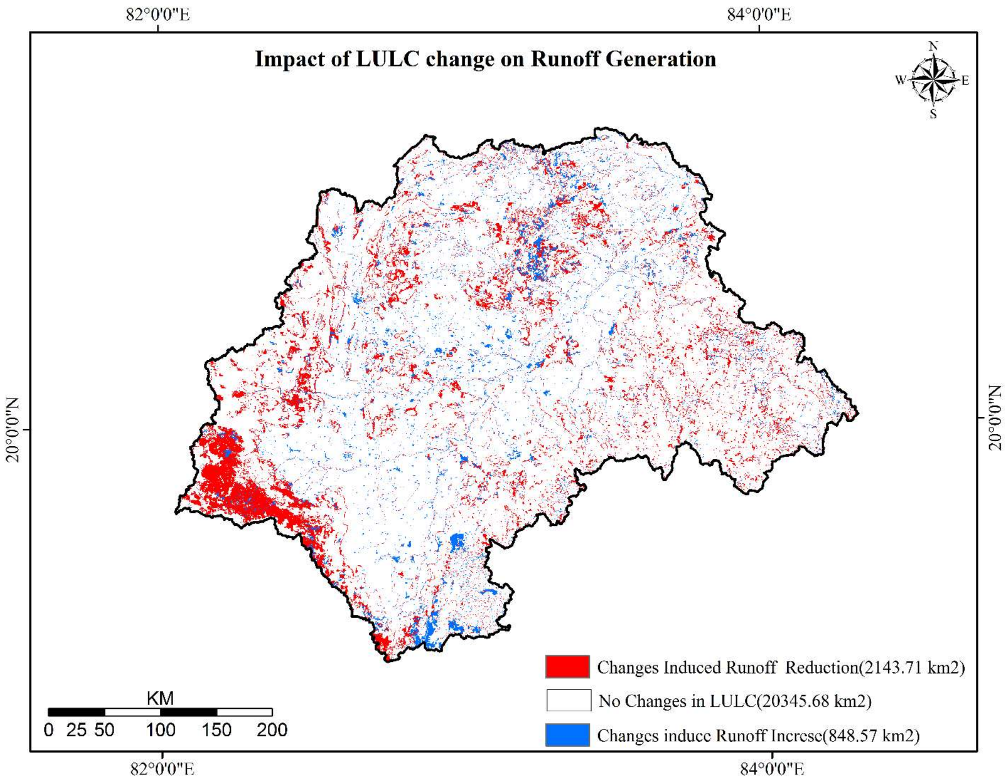

Figure 6. Impact of LULC change on runoff generation

4. CONCLUSION

The analysis of Land Use and Land Cover (LULC) dynamics in the Tel basin provides a robust foundation for understanding hydrological responses. Decadal mapping, employing advanced Machine Learning (ML) techniques, revealed an 8.20% decline in forest cover over 30 years, mainly due to deforestation (1,600 km^2 converted to agriculture). This transformation significantly impacted runoff, contributing to a noteworthy increase of 67.33 mm at pixel level. The consistent rise in runoff potential, coupled with a 167.48 mm decrease in evapotranspiration (at pixel level), underscores the intricate link between land cover changes and hydrological dynamics. Scenario-based analysis highlights the cumulative impact of urbanization and deforestation on increased runoff, emphasizing the need for sustainable land management. The observed anomaly in baseflow underscores the intricate relationship between land use modifications and subsurface flow. These findings have broader implications, emphasizing the delicate balance between anthropogenic activities and hydrological processes, necessitating informed land management decisions for watershed resilience in the face of environmental challenges. Future considerations should involve predictive modeling and climate change scenarios to anticipate potential shifts in LULC and their hydrological impacts. In conclusion, the findings underscore the critical role of informed land management decisions, especially in regions experiencing dynamic land use changes. Forest preservation emerges as a linchpin for sustaining a balanced and resilient water cycle within the Tel sub-basin. This scientific exploration contributes to the broader understanding of human-induced impacts on hydrological dynamics and underscores the imperative for sustainable watershed management practices.

References

Abdulla, Fayez A, Dennis P Lettenmaier, Eric F Wood, and James A Smith. 1996. Application of a Macroscale Hydrologic Model to Estimate the Water Balance of the Arkansas-Red River Basin. Journal of Geophysical Research: Atmospheres 101 (D3): 7449–59. https://doi.org/https://doi.org/10.1029/95JD02416.

Aboelnour, Mohamed A, Bernard A Engel, Marty D Frisbee, Margaret W Gitau, and Dennis C Flanagan. 2021. Impacts of Watershed Physical Properties and Land Use on Baseflow at Regional Scales. Journal of Hydrology: Regional Studies 35: 100810. https://doi.org/https://doi.org/10.1016/j.ejrh.2021.100810.

Aggarwal, S. P., V. Garg, P. K. Gupta, B. R. Nikam, and P. K. Thakur. 2012. Climate and Lulc Change Scenarios To Study Its Impact on Hydrological Regime. The International Archives of the Photogrammetry, Remote Sensing and Spatial Information Sciences XXXIX-B8 (September): 147–52. https://doi.org/10.5194/isprsarchives-xxxix-b8-147-2012.

Aggarwal, S.P., Garg, V., Gupta, P.K., Nikam, B.R., Thakur, P.K. and Roy P.S. (2013). Runoff potential assessment over Indian landmass: A macro-scale hydrological modeling approach. Current Science, 104(7), 950-959.

Aggarwal, S.P., Thakur, P. K., Garg, V., Nikam, B. R., Chouksey, A., Dhote, P. and Bhattacharya, T. (2016). Water Resources Status and Availability Assessment in Current and Future Climate Change Scenarios for Beas River Basin of North Western Himalaya. The International Archives of the Photogrammetry, Remote Sensing and Spatial Information Sciences (ISPRS), XLI-B8 2016, XXIII ISPRS Congress, 12–19 July 2016, Prague, Czech Republic, 1389-1396. doi:10.5194/isprs-archives-XLI-B8-1389-2016

Behera, M. D., P. Tripathi, P. Das, S. K. Srivastava, P. S. Roy, C. Joshi, P. R. Behera, et al. 2018. Remote Sensing Based Deforestation Analysis in Mahanadi and Brahmaputra River

Basin in India since 1985. Journal of Environmental Management 206: 1192–1203. https://doi.org/10.1016/j.jenvman.2017.10.015.

Behera, S. S., Nikam, B. R. and Babel, M. S. (2017). Assimilation of Remotely Sensed Soil Moisture into Hydrological Model: A Case Study of Mahanadi Basin, India. In Proceedings of ACRS 2017: 38th Asian Conference on Remote Sensing organized at New Delhi, India, October 23-27, 2017.

Berihun, Mulatu Liyew, Atsushi Tsunekawa, Nigussie Haregeweyn, Derege Tsegaye Meshesha, Enyew Adgo, Mitsuru Tsubo, Tsugiyuki Masunaga, et al. 2019. Hydrological Responses to Land Use/Land Cover Change and Climate Variability in Contrasting Agro-Ecological Environments of the Upper Blue Nile Basin, Ethiopia. Science of The Total Environment 689: 347–65. https://doi.org/https://doi.org/10.1016/j.scitotenv.2019.06.338.

Chandu, Navya, T I Eldho, and Arpita Mondal. 2022. Hydrological Impacts of Climate and Land-Use Change in Western Ghats, India. Regional Environmental Change 22 (1): 32. https://doi.org/10.1007/s10113-022-01879-2.

Chen, Yuyao, Jun Niu, Shaozhong Kang, and Xiaotao Zhang. 2018. Effects of Irrigation on Water and Energy Balances in the Heihe River Basin Using VIC Model under Different Irrigation Scenarios. Science of The Total Environment 645: 1183–93. https://doi.org/https://doi.org/10.1016/j.scitotenv.2018.07.254.

Cherkauer, Keith A, Laura C Bowling, and Dennis P Lettenmaier. 2003. Variable Infiltration Capacity Cold Land Process Model Updates. Global and Planetary Change 38 (1): 151–59. https://doi.org/https://doi.org/10.1016/S0921-8181(03)00025-0.

Cuo, Lan, Yongxin Zhang, Yanhong Gao, Zhenchun Hao, and Luosang Cairang. 2013. The Impacts of Climate Change and Land Cover/Use Transition on the Hydrology in the Upper Yellow River Basin, China. Journal of Hydrology 502: 37–52. https://doi.org/https://doi.org/10.1016/j.jhydrol.2013.08.003.

Dadhwal, V K, S P Aggarwal, and Nidhi Mishra. 2010. Hydrological Simulation of Mahanadi River Basin and Impact of Land Use / Land Cover Change On Surface Runoff Using a Macro Scale Hydrological Model. In .

Dahri, Zakir Hussain, Fulco Ludwig, Eddy Moors, Shakil Ahmad, Bashir Ahmad, Sarfraz Ahmad, Muhammad Riaz, and Pavel Kabat. 2021. Climate Change and Hydrological Regime of the High-Altitude Indus Basin under Extreme Climate Scenarios. Science of The Total Environment 768: 144467. https://doi.org/https://doi.org/10.1016/j.scitotenv.2020.144467.

Das, Pulakesh, Mukunda Dev Behera, Nitesh Patidar, Bhabagrahi Sahoo, Poonam Tripathi, Priti Ranjan Behera, S. K. Srivastava, et al. 2018. Impact of LULC Change on the Runoff, Base Flow and Evapotranspiration Dynamics in Eastern Indian River Basins during 1985–2005 Using Variable Infiltration Capacity Approach. Journal of Earth System Science 127 (2): 1–19. https://doi.org/10.1007/s12040-018-0921-8.

Dixit, A., Nikam, B. R., Aggarwal, S. P., Garg, V., Gupta, P.K. and Thakur, P. K. (2015). Runoff Estimation for forthcoming years of Chambal River Basin, Using VIC and ARIMA Model. In Proceedings of ‘HYDRO 2015 INTERNATIONAL’, 20th International Conference on Hydraulics, Water Resources and River Engineering organized at IIT Roorkee, India, 17-19 December, 2015.

Garg, V, S P Aggarwal, B R Nikam, and P K Thakur. 2013. Hypothetical Scenario–Based Impact Assessment of Climate Change on Runoff Potential of a Basin. ISH Journal of Hydraulic Engineering 19 (3): 244–49. https://doi.org/10.1080/09715010.2013.804673.

Garg, V., Dhumal, I. R., Nikam, B. R., Thakur, P. K., Aggarwal, S.P., Srivastav, S.K. and Senthil Kumar, A. (2016). Water Resources Assessment of Godavari River Basin, India. In Proceedings of ACRS 2016: 37th Asian Conference on Remote Sensing organized at Colombo, Sri Lanka, during October, 17-21, 2016.

Garg, Vaibhav, Ampha Khwanchanok, P K Gupta, Shyam Aggarwal, Komsan Kiriwongwattana, Praveen Kumar Thakur, and Bhaskar Ramchandra Nikam. 2012. Urbanisation Effect on Hydrological Response: A Case Study of Asan River Watershed, India. Journal of Environment and Earth Science 2: 39–50.

Garg, Vaibhav, Bhaskar Ramchandra Nikam, Praveen Kumar Thakur, Shiv Prasad Aggarwal, Prasun Kumar Gupta, and Sushil Kumar Srivastav. 2019. Human-Induced Land Use Land Cover Change and Its Impact on Hydrology. HydroResearch 1: 48–56. https://doi.org/10.1016/j.hydres.2019.06.001.

Garg, Vaibhav, Rohit S. Sambare, Praveen K. Thakur, Pankaj R. Dhote, Bhaskar R. Nikam, and S. P. Aggarwal. 2019. Improving Stream Flow Estimation by Incorporating Time Delay Approach in Soft Computing Models. ISH Journal of Hydraulic Engineering 00 (00): 1–12. https://doi.org/10.1080/09715010.2019.1676171.

Garg, Vaibhav, S P Aggarwal, Prasun K Gupta, Bhaskar R Nikam, Praveen K Thakur, S K Srivastav, and A Senthil Kumar. 2017. Assessment of Land Use Land Cover Change Impact on Hydrological Regime of a Basin. Environmental Earth Sciences 76 (18): 635. https://doi.org/10.1007/s12665-017-6976-z.

Gashaw, Temesgen, Taffa Tulu, Mekuria Argaw, and Abeyou W Worqlul. 2018. Modeling the Hydrological Impacts of Land Use/Land Cover Changes in the Andassa Watershed, Blue Nile Basin, Ethiopia. Science of The Total Environment 619–620: 1394–1408. https://doi.org/https://doi.org/10.1016/j.scitotenv.2017.11.191.

Ghimire, Usha, Sangam Shrestha, Sanjiv Neupane, S Mohanasundaram, and Oranuj Lorphensri. 2021. Climate and Land-Use Change Impacts on Spatiotemporal Variations in Groundwater Recharge: A Case Study of the Bangkok Area, Thailand. Science of The Total Environment 792: 148370. https://doi.org/https://doi.org/10.1016/j.scitotenv.2021.148370.

Guru, Nibedita, and Ramakar Jha. 2015. Flood Frequency Analysis of Tel Basin of Mahanadi River System, India Using Annual Maximum and POT Flood Data. Aquatic Procedia 4: 427–34. https://doi.org/https://doi.org/10.1016/j.aqpro.2015.02.057.

Haddeland, Ingjerd, Thomas Skaugen, and Dennis P Lettenmaier. 2006. Anthropogenic Impacts on Continental Surface Water Fluxes. Geophysical Research Letters 33 (8). https://doi.org/https://doi.org/10.1029/2006GL026047.

Hengade, Narendra, and T I Eldho. 2019. Relative Impact of Recent Climate and Land Cover Changes in the Godavari River Basin, India. Journal of Earth System Science 128 (4): 94. https://doi.org/10.1007/s12040-019-1135-4.

Keerthiga, J., Nikam, B. R., Garg, V., Thakur, P. K., Gupta, P. K., Chouksey, A., Aggarwal, S. P., Srivastav, S. K. and Senthil Kumar, A. (2017). Climate Change Impact Assessment on Hydrological Regime of Krishna Basin. In Proceedings of ACRS 2017: 38th Asian Conference on Remote Sensing organized at New Delhi, India, October 23-27, 2017.

Kumari, Nikul, Ankur Srivastava, Bhabagrahi Sahoo, Narendra Singh Raghuwanshi, and David Bretreger. 2021. Identification of Suitable Hydrological Models for Streamflow Assessment in the Kangsabati River Basin, India, by Using Different Model Selection Scores. Natural Resources Research 30 (6): 4187–4205. https://doi.org/10.1007/s11053-021-09919-0.

Lee, Jaehyeong, Yeonjoo Kim, and Dagang Wang. 2022. Assessing the Characteristics of Recent Drought Events in South Korea Using WRF-Hydro. Journal of Hydrology 607: 127459. https://doi.org/https://doi.org/10.1016/j.jhydrol.2022.127459.

Liang, Xu, D. P. Lettenmaier, E. F. Wood, and S. J. Burges. 1994. A Simple Hydrologically Based Model of Land Surface Water and Energy Fluxes for General Circulation Models. Journal of Geophysical Research 99 (D7). https://doi.org/10.1029/94jd00483.

Liang, Xu, Eric F Wood, and Dennis P Lettenmaier. 1996. Surface Soil Moisture Parameterization of the VIC-2L Model: Evaluation and Modification. Global and Planetary Change 13 (1): 195–206. https://doi.org/https://doi.org/10.1016/0921-8181(95)00046-1.

Lohmann, D, E Raschke, and D P Lettenmaier. 1998. Regional Scale Hydrology: I. Formulation of the VIC-2L Model Coupled to a Routing Model. Hydrological Sciences Journal 43 (1): 131–41. https://doi.org/10.1080/02626669809492107.

Matlhodi, Botlhe, Piet K Kenabatho, Bhagabat P Parida, and Joyce G Maphanyane. 2021. Analysis of the Future Land Use Land Cover Changes in the Gaborone Dam Catchment Using CA-Markov Model: Implications on Water Resources. Remote Sensing . https://doi.org/10.3390/rs13132427.

Maurer, E P, A W Wood, J C Adam, D P Lettenmaier, and B Nijssen. 2002. A Long-Term Hydrologically Based Dataset of Land Surface Fluxes and States for the Conterminous United States. Journal of Climate 15 (22): 3237–51. https://doi.org/10.1175/1520-0442(2002)015<3237:ALTHBD>2.0.CO;2.

Mishra, S Sangita, and R Nagarajan. 2011. Spatio-Temporal Drought Assessment in Tel River Basin Using Standardized Precipitation Index (SPI) and GIS. Geomatics, Natural Hazards and Risk 2 (1): 79–93. https://doi.org/10.1080/19475705.2010.533703.

Naha, S, M A Rico-Ramirez, and R Rosolem. 2021. Quantifying the Impacts of Land Cover Change on Hydrological Responses in the Mahanadi River Basin in India. Hydrology and Earth System Sciences 25 (12): 6339–57. https://doi.org/10.5194/hess-25-6339-2021.

Niemeyer, Ryan J, Yifan Cheng, Yixin Mao, John R Yearsley, and Bart Nijssen. 2018. A Thermally Stratified Reservoir Module for Large-Scale Distributed Stream Temperature

Models With Application in the Tennessee River Basin. Water Resources Research 54 (10): 8103–19. https://doi.org/https://doi.org/10.1029/2018WR022615.

Nijssen, Bart, Dennis P Lettenmaier, Xu Liang, Suzanne W Wetzel, and Eric F Wood. 1997. Streamflow Simulation for Continental-Scale River Basins. Water Resources Research 33 (4): 711–24. https://doi.org/https://doi.org/10.1029/96WR03517.

Nijssen, Bart, Reiner Schnur, and Dennis P Lettenmaier. 2001. Global Retrospective Estimation of Soil Moisture Using the Variable Infiltration Capacity Land Surface Model, 1980–93. Journal of Climate 14 (8): 1790–1808. https://doi.org/10.1175/1520-0442(2001)014<1790:GREOSM>2.0.CO;2.

Nikam, Bhaskar Ramchandra, Vaibhav Garg, Keerthiga Jeyaprakash, Prasun Kumar Gupta, Sushil Kumar Srivastav, Praveen Kumar Thakur, and Shiv Prasad Aggarwal. 2018. Analyzing Future Water Availability and Hydrological Extremes in the Krishna Basin under Changing Climatic Conditions. Arabian Journal of Geosciences 11 (19). https://doi.org/10.1007/s12517-018-3936-1.

Niu, Jun, Ji Chen, and Liqun Sun. 2015. Exploration of Drought Evolution Using Numerical Simulations over the Xijiang (West River) Basin in South China. Journal of Hydrology 526: 68–77. https://doi.org/https://doi.org/10.1016/j.jhydrol.2014.11.029.

Patidar, N, and M D Behera. 2019. How Significantly Do Land Use and Land Cover (LULC) Changes Influence the Water Balance of a River Basin? A Study in Ganga River Basin, India. Proceedings of the National Academy of Sciences, India Section A: Physical Sciences 89 (2): 353–65. https://doi.org/10.1007/s40010-017-0426-x.

Sharma, V., Nikam, B. R., Thakur, P. K., Garg, V., and Aggarwal, S. P. (2019). Effect of Bias Correction in Era-Interim Precipitation Dataset on the Behaviour of Hydrological Model. In Proceedings of 'HYDRO 2019 INTERNATIONAL', 24th International Conference on Hydraulics, Water Resources, Coastal & Environmental Engineering, December 18-20, 2019, At Osmania University, Hyderabad, India.

Shayeghi, Afshin, Asghar Azizian, and Luca Brocca. 2020. Reliability of Reanalysis and Remotely Sensed Precipitation Products for Hydrological Simulation over the Sefidrood River Basin, Iran. Hydrological Sciences Journal 65 (2): 296–310. https://doi.org/10.1080/02626667.2019.1691217.

Shiradhonkar, S., Garg, V., Nikam, B. R., Thakur, P. K. and Aggarwal, S. P. (2015). Hydrological Modelling of a Large River Basin Using Geospatial Tools. In Proceedings of 'HYDRO 2015 INTERNATIONAL', 20th International Conference on Hydraulics, Water Resources and River Engineering organized at IIT Roorkee, India, 17-19 December, 2015.

Shrestha, Rajesh R, Markus A Schnorbus, Arelia T Werner, and Anne J Berland. 2012. Modelling Spatial and Temporal Variability of Hydrologic Impacts of Climate Change in the Fraser River Basin, British Columbia, Canada. Hydrological Processes 26 (12): 1840–60. https://doi.org/https://doi.org/10.1002/hyp.9283.

Sinha, Rakesh Kumar, T I Eldho, and Ghosh Subimal. 2020. Assessing the Impacts of Land Cover and Climate on Runoff and Sediment Yield of a River Basin. Hydrological Sciences Journal 65 (12): 2097–2115. https://doi.org/10.1080/02626667.2020.1791336.

Su, F, L Zhang, T Ou, D Chen, T Yao, K Tong, and Y Qi. 2016. Hydrological Response to Future Climate Changes for the Major Upstream River Basins in the Tibetan Plateau. Global and Planetary Change 136: 82–95. https://doi.org/https://doi.org/10.1016/j.gloplacha.2015.10.012.

Tavakoly, Ahmad A, Alan D Snow, Cédric H David, Michael L Follum, David R Maidment, and Zong-Liang Yang. 2017. Continental-Scale River Flow Modeling of the Mississippi River Basin Using High-Resolution NHDPlus Dataset. JAWRA Journal of the American Water Resources Association 53 (2): 258–79. https://doi.org/https://doi.org/10.1111/1752-1688.12456.

Verma, Narender, Ramesh Kumar Patel, and Pandurang Choudhari. 2022. Watershed Prioritization for Soil Conservation in a Drought Prone Watershed of Eastern India: Tel River Basin, Odisha. Geology, Ecology, and Landscapes, January, 1–14. https://doi.org/10.1080/24749508.2021.2022830.

Vetter, T, S Huang, V Aich, T Yang, X Wang, V Krysanova, and F Hattermann. 2015. Multi-Model Climate Impact Assessment and Intercomparison for Three Large-Scale River Basins on Three Continents. Earth System Dynamics 6 (1): 17–43. https://doi.org/10.5194/esd-6-17-2015.

Voisin, Nathalie, Florian Pappenberger, Dennis P Lettenmaier, Roberto Buizza, and John C Schaake. 2011. Application of a Medium-Range Global Hydrologic Probabilistic Forecast Scheme to the Ohio River Basin. Weather and Forecasting 26 (4): 425–46. https://doi.org/10.1175/WAF-D-10-05032.1.

Wang, Ning, Wenbin Liu, Hong Wang, Fubao Sun, Weili Duan, Zehua Li, Zhi Li, and Yaning Chen. 2021. Improving Streamflow and Flood Simulations in Three Headwater Catchments of the Tarim River Based on a Coupled Glacier-Hydrological Model. Journal of Hydrology 603: 127048. https://doi.org/https://doi.org/10.1016/j.jhydrol.2021.127048.

Zamani Sabzi, Hamed, Hernan A Moreno, Rachel Fovargue, Xianwu Xue, Yang Hong, and Thomas M Neeson. 2019. Comparison of Projected Water Availability and Demand Reveals Future Hotspots of Water Stress in the Red River Basin, USA. Journal of Hydrology: Regional Studies 26: 100638. https://doi.org/https://doi.org/10.1016/j.ejrh.2019.100638.